Hindawi
Journal of Nanomaterials
Volume 2022, Article ID 8211023, 13 pages
https://doi.org/10.1155/2022/8211023

*Research Article*

# Modeling Energy Gap of Doped Tin (II) Sulfide Metal Semiconductor Nanocatalyst Using Genetic Algorithm-Based Support Vector Regression

**Peter Chibuike Okoye,[1,2] Samuel Ogochukwu Azi,[2] Taoreed O. Owolabi,[1] Oke Wasiu Adeyemi,[3] Miloud Souiyah,[4] Mouftahou B. Latif,[5,6] and Olubosede Olusayo[7]**

[1]*Physics and Electronics Department, Adekunle Ajasin University, Akungba Akoko, 342111 Ondo State, Nigeria*
[2]*Department of Physics, University of Benin, Benin City, Edo State, Nigeria*
[3]*Department of Mechanical and Mechatronics Engineering, Afe Babalola University Ado-Ekiti, P.M.B 5454, Ado Ekiti, Nigeria*
[4]*Department of Mechanical Engineering, College of Engineering, University of Hafr Al Batin, P.O. Box 1803, Hafr Al Batin 31991, Saudi Arabia*
[5]*Centre for Energy Research and Development, Obafemi Awolowo University, Ile-Ife 220005, Nigeria*
[6]*KU Leuven, Instituut voor Kern- en Stralingsfysica, B-3001 Leuven, Belgium*
[7]*Physics Department, Federal University Oye Ekiti, Oye Ekiti, Ekiti State, Nigeria*

Correspondence should be addressed to Taoreed O. Owolabi; owolabitaoreedolakunle@gmail.com

Received 7 December 2021; Accepted 3 May 2022; Published 17 May 2022

Academic Editor: Palanivel Velmurugan



Tin (II) sulfide (SnS) is a metal chalcogenide semiconducting material with fascinating and admirable physical features for practical applications in solid-state batteries, photodetectors, gas sensors, optoelectronic devices, emission transistors, and photocatalysis among others. The energy gap of SnS semiconductor nanomaterial that facilitates its usefulness in many applications can be adjusted through dopant incorporation which results in crystal lattice distortion at various crystallite sizes of the semiconductor. This work employs lattice parameter descriptors to develop a hybrid genetic algorithm (GA) and support vector regression algorithm (SVR) intelligent model for determining the energy gap of doped SnS semiconductors. The predictive strength of the developed GA-SVR model is compared with the stepwise regression algorithm- (STRA-) based model using different performance evaluation parameters. The developed GA-SVR model performs better than STRA model based on root mean square error, mean absolute error, and correlation coefficient with performance improvement of 70.68%, 67.63%, and 20.98%, respectively, using the testing set of data. Influence of different dopants and experimental conditions on energy gap of SnS semiconductor were investigated using the developed model, while the obtained values for the energy gaps agree with the measured values. The developed models demonstrate high degree of potentials in terms of accuracy, precision, and ease of implementation that fosters their real-life applicability in estimating the energy gap of doped SnS semiconductor with experimental stress circumvention.

## 1. Introduction

The harmful impact of fossil fuel energy on our environment has prompted researchers to turn their attention to renewable energy sources such as sunlight to address the demand for a sustainable and inexpensive clean energy source [1, 2]. Photovoltaic thin films obtained from environmentally friendly materials are needed to harness the energy from sunlight [3, 4]. Examples of such materials are the metal chalcogenide thin films which include CdS, CdTe, $Cu_2S$, CIS, CZTS, SnS, and CIGS among others. Metal chalcogenides are materials with the potentials for future success in many different fields [5–7]. Among these materials, SnS has earned a lot of interest as an absorbing

thin-film photovoltaic layer because of its optical, chemical, electrical, and physical properties that are better than or can be compared with those of other materials [8, 9]. Its elemental components (Sn and S) are inexpensive, naturally available, and harmless [10]. Out of all the compounds of tin sulfide, SnS is found to exhibit unique properties and can be used in thin-film heterojunction solar cell fabrication [11], optoelectronic devices, near-infrared (NIR) photodetectors, absorber layer, solid-state batteries, holographic recording, capacitors, gas sensors, electrical switching, photocatalysts, field emission transistors, and drug delivery devices as a result of its simple growth chemistry, high stability, natural abundance, and low toxicity [12, 13]. The optical energy gap of this semiconductor that enhances its diverse applications is characterized and modeled in this contribution using hybrid intelligent and stepwise regression-based algorithms.

Tin (II) sulfide (SnS) is one of the binary compounds that fit into groups IV to VI metal chalcogenide semiconductors with layered structures. These compounds exhibit meaningful variations in their physical properties such as absorbance and electrical and thermal conductivities when taking measurements along their crystallographic axes because of the presence of layers in their structures [14]. In SnS compound, six atoms of S are attached to each atom of Sn through van der Waals bonding [15]. Tin (II) sulfide is found to exist in various forms as SnS, SnS2, Sn2S3, Sn3S4, and Sn4S5 [16]. Being a p-type semiconductor material, SnS has an enhanced direct energy band gap that is widely used in photovoltaic applications as a result of its high absorption coefficient (greater than $10^4\,cm^{-1}$) [17]. It has a direct optical energy band gap ranging from 1.2 eV to 1.5 eV [18, 19] and an indirect optical energy band gap of 1 eV to 1.2 eV [20]. Its high free carrier concentration of $10^{15}\,cm^{-3}$ makes it an important material for many oxide reduction systems [21]. Experimental efficiency values for SnS-based solar cells are found to fall short of theoretical projections. The theoretical photoconversion efficiency limit of SnS-based solar cells is found to be between 25% and 30% [22], whereas the efficiency from experiments is found to be between 4% and 5% [23, 24]. The reason for reduced theoretical photoconversion efficiency can be attributed to short carrier lifetime, band alignment and offset, diffusion length, crystalline lattice defects, presence of other tin sulfide phases [10, 25], reduced purity, and fabrication flaws [26, 27]. The performance of SnS as a material for absorbing solar energy can be enhanced by doping with Bi [28, 29], Ag [30, 31], Al [32], Fe [33], Cu [34], Sb [35, 36], Ge [37], In [30, 31], and Pb [38]. Different techniques have been reportedly employed in synthesizing SnS thin films. The techniques includes electron beam evaporation [39], molecular beam epitaxy [40], electrodeposition (ED) [41–45], vacuum evaporation [46, 47], atomic layer deposition (ALD) [48], sputtering [49], multilayer-based solid-state reaction [50], plasma-enhanced chemical vapour deposition (PECVD) [51], hot well vacuum deposition (HWVD) [52], chemical bath deposition (CBD) [53–58], chemical spray pyrolysis, [59–64], successive ionic layer adsorption and reaction (SILAR) [65–67], and brush plating [68]. The need for a computational method of energy gap characterization becomes significant since experimental synthesis as well as characterization of SnS semiconductor is laborious, time-consuming, and costly. This work employs a stepwise regression-based algorithm and hybridization of genetic algorithm (GA) with support vector regression algorithm. Distorted lattice parameters are used as descriptors to the models.

Support vector regression (SVR) is a machine learning algorithm that learns and models linear as well as nonlinear relationships between a dependent variable (known as target) and independent variables (known as descriptors) [69]. SVR algorithm has the uniqueness of converging to the very least minimum error even if it has a small number of training samples [70]. This uniqueness stands SVR out among other machine learning techniques such as artificial neural network which shows better performance when trained with lager number of samples [71–73]. However, neural network and other machine learning techniques have demonstrated superior performance in handling most difficult trend [74–76]. SVR algorithm is a support vector machine classifier extension that converts input data to higher-dimensional feature space and performs linear regression in that space [77]. Its special feature is its ability to solve nonlinear problems using kernel trick [78]. This distinctive characteristic of the algorithm, along with other inherent properties including its ability to easily converge to global solutions and a solid background in mathematics, has been harnessed in various applications [79–81]. The existence of constraints, which are the conditions of convex optimization problems, is responsible for the observed global minimum convergence [82]. To improve the efficiency of the prediction of SVR algorithm, SVR hyperparameters are enhanced through optimization. In this study, genetic algorithm (GA) is used to enhance SVR hyperparameters to have a more robust hybrid model for predicting the energy gap of tin (II) sulfide semiconductor.

Genetic algorithm is an optimization algorithm based on Charles Darwin's theory of natural selection [83]. It involves the selection of the fittest individuals from a given population to produce the best offspring for the next generations. The offspring of these individuals will have characteristics similar to the parents. If parents have the best fitness levels, their offspring will be better than them [84]. This process repeats itself until the best fit individuals are found. This concept can be used to solve a search problem through a set of solutions that are selected from a selection of the best ones. The steps that are considered in a genetic algorithm are initial population generation, fitness function computation, selection, crossover, elitism, and mutation operation.

The rest of the manuscript is organized as follows: Section 2 contains the formulation of the proposed hybrid support vector regression and genetic algorithm. Section 3 contains a description of the dataset and the computational methodology of the proposed hybrid algorithm. The results of the proposed hybrid model and comparisons to the results of other developed model are discussed in Section 4. Section 5 contains the conclusion to the study.

## 2. Mathematical Formulation and Background

The mathematical formulation of the support vector regression algorithm and the applied genetic optimization technique is presented in this section. In addition, the background of the stepwise regression algorithm is also discussed.

*2.1. Support Vector Regression.* As a computational intelligence method, support vector regression (SVR) is developed based on the statistical learning theory for solving regression problems [82]. SVR evolves from the support vector machine (SVM) initially formulated to solve classification problems [85, 86]. Several SVM implementations have been achieved in different research areas after formulation [87, 88]. SVM is therefore a universal term that is subdivided into support vector classification (SVC) and support vector regression (SVR) [86]. SVR is developed based on SVM elements, in which support vectors are primarily closer points towards the algorithm hyperplane in an n-dimensional feature space that separates the data points around the hyperplane [89]. It is a supervised learning approach that uses the kernel trick to transfer observed data to a target variable [90]. To develop a predictive model, SVR makes use of a collection of training data that contains predictor variables as well as their corresponding observed responses. By relying solely on the predictor variables, the resulting SVR model can accurately generalize to future unknown data [91]. SVR is based on sound mathematical theory and its optimization problem has an optimal and global solution in the form of linearly constrained quadratic programming [92]. Linear regression constructed with SVR is generally defined as contained in

$$f(x,\propto) = \langle w, x\rangle + b, \tag{1}$$

where $w \epsilon K$ and $b \epsilon \mathbb{R}$.

The purpose of SVR is to determine $w$ vector and bias $b$ such that for all training datasets, the defined error threshold epsilon $\varepsilon$ is not exceeded. To ensure adequate SVR training and flatness, the constrained equations governing the operational implementation of SVR algorithm, vector $\omega$ should be minimized while the minimization of the Euclidean norm $\|w\|^2$ should be obtained by a transformation to a convex optimization problem as revealed in

$$\begin{aligned} &\text{Minimize}\frac{1}{2}\|w\|^2 \\ &\text{Subject to}\begin{cases} y_i - \langle w, x_i\rangle - b \le \varepsilon \\ \langle w, x_i\rangle + b - y_i \le \varepsilon \end{cases} \end{aligned} \tag{2}$$

Constraints that may prevent the possibility and feasibility of the convex optimization problem in equation (2) are factored in through slack variables ($\xi_i$ and $\xi_i^*$) inclusion. The optimization problem is further transformed as reported in

$$\begin{aligned} &\text{Minimize}\frac{1}{2}\|w\|^2 + C\sum_{i=1}^{i}\left(\xi_i + \xi_i^*\right) \\ &\text{Subject to}\begin{cases} y_i - \langle w, x_i\rangle - b \le \varepsilon + \xi_i \\ \langle w, x_i\rangle + b - y_i \le \varepsilon + \xi_i^* \\ \xi_i, \xi_i^* \ge 0 \end{cases} \end{aligned} \tag{3}$$

where $C$ is the regularization or penalty factor.

Regularization or penalty factor $C$, kernel function parameter, and the epsilon parameter $\varepsilon$ are all user-defined parameters that significantly influence the SVR model general performance. The penalty factor $C$ controls the existing difference between training data error tolerance and model complexity. The number of support vectors in insensitive zones is determined by the epsilon parameter, while the kernel function parameter controls the transfer of the input data to a feature space of higher dimension. [93, 94].

*2.2. Genetic Algorithm.* Genetic algorithm (GA) is a type of random optimization approach that belongs to the family of heuristic evolutionary computational algorithms motivated by Darwin's theory of evolution [95, 96]. GA consists of three operations after fitness evaluation and computation: selection, crossover, and mutation. If all three operations remain constant throughout the algorithm, it is referred to as a simple genetic algorithm [83]. GA begins with no knowledge of the optimal solution and relies entirely on environmental responses to find the best solution by utilizing evolutionary principles [97]. Application of GA starts from a population containing individual data structures that resemble chromosomes, which consists of genes that encode the individual's hereditary characters that can be reproduced when running the algorithm [98–100]. After that, each chromosome is decoded and assigned a fitness criterion as well as a fitness number using the root mean square error metric. The probability of selection of each individual is determined by the assigned fitness number [101]. Every new member goes through the same process. Genetic algorithm operators which include crossover, mutation, and selection are utilized in generating subsequent generations. This procedure is repeated until the convergence requirement is met.

*2.3. Stepwise Regression.* As a multiple linear regression technique, stepwise regression helps in finding the optimum combination of independent variables for predicting the dependent variable by incrementally adding or removing variables [102]. With significantly less processing than is required for all conceivable regressions, stepwise regression is a reliable approach for selecting the right subset models or the right set of independent variables that is the most suitable for the dependent variable [103]. Subset models are determined by adding and deleting variables that have maximum influence on the residual sum of squares. Selection of variables can be in forward, backward, or a combination of

both directions. Forward selection involves a successive addition of variables to a subset that has already been chosen. Each step adds to the subset a variable from the variables in the subset that is absent in the model that generates maximum reduction in the residual sum of squares. Forward selection continues with no termination condition till every variable is included in the model. Backward stepwise variable selection starts by choosing the subset models from the complete model and removing every variable whose removal at each step will minimally increase the residual sum of squares and continue till one variable is contained in the subset model. It should be noted that when using forward and backward techniques, the impact of the addition or removal of a variable on the inputs of other variables to the model is not taken into account. As a result, stepwise regression rechecks the significance of all previously added variables at each step. If the partial sums of squares of any earlier added variables do not reach a minimal condition to remain in the model, the selection process switches to backward elimination, with variables being discarded one by one till the minimal requirement is met by all remaining variables. The variable selection procedure is complete when every variable within the model fulfills the requirement to remain and no variables outside the model have the entry requirement.

## 3. Computational Methodology of the Proposed Hybrid GA-SVR

Details of the data employed for the simulation and modeling as well as the methods used for combining SVR and GA into a robust hybrid model are discussed in the present section.

*3.1. Description of the Employed Set of Data for Simulation.* The lattice parameters of doped forty-one samples of SnS semiconductors were employed in establishing an intelligent-based relationship through which energy gap of the semiconductor nanocatalyst could be determined. The experimental data for model development and validation was extracted from the literature [30, 104–110]. Aside from doping, an experimental condition such as annealing temperature influences the dislocation density as well as the sample microstrain with ultimate impact on the sample lattice parameters. The employed data for simulation and modeling is statistically analyzed and presented in Table 1.

The obtained coefficients of correlation between each of the model predictors and the energy gap strongly indicate the presence of a very weak linear relationship between lattice parameters ($a$, $b$, and $c$) and energy gap despite the physically established influence of dopants on SnS lattice parameters and energy gap [30]. Hence, the need for the proposed hybrid intelligent-based algorithms becomes necessary. The presented mean and maximum values for each descriptor as well as the energy gap further enhance insightful information from the employed data such as the dataset content, while the presented standard deviations allow useful information about the experimental consistencies in the acquired set of data.

Table 1: Statistical analysis of the employed set of data.

| Statistical parameters | $a$ (Å) | $b$ (Å) | $c$ (Å) | Eg (eV) |
|---|---|---|---|---|
| Mean | 4.30 | 11.19 | 3.94 | 1.35 |
| Correlation coefficient | -0.17 | -0.14 | 0.14 | 1.00 |
| Maximum | 4.79 | 11.48 | 4.24 | 1.88 |
| Standard deviation | 0.18 | 0.18 | 0.17 | 0.19 |

*3.2. Computational Description of the Proposed Hybrid Intelligent-Based Algorithms.* The whole computing task involving hybridizing SVR with GA was carried out on MATLAB. All the datasets were first randomized to provide a regular distribution of data points and to improve the models' computational efficiency before the start of simulation. Randomization is the process of strategically splitting a dataset into training and testing set to prevent a situation where the training and testing samples are biased, resulting in testing the model on what it has not been trained to learn. The implemented splitting ratio for the training and testing sets for this work is 8 : 2. Genetic algorithm assists in hyperparameter searching and, as a result, improves the accuracy and strength of the model. The hyperparameters optimized by the genetic algorithm are the kernel option, epsilon, and penalty or regularization factor. The stepwise descriptions of the computing strategies for the hybridized GA-SVR model are itemized as follows:

Step I. Initialization and generalization of population size: a random generation of several individual solutions is used to initiate a specific number of initial populations. The size of the initially created population is determined by the description of the problem as well as the scope of the search space

Step II. Evaluation of possible solutions: the evaluation of the probable solution of the initially generated population is achieved by using the fitness function to determine the strength of the solution using the root mean square error (RMSE). A solution with the least RMSE value indicates the maximum measure of fitness and vice versa. Procedures for the evaluation of fitness are listed below:

(a) Selection of kernel function: select a kernel function from Gaussian, Sigmoid, or polynomial function

(b) Every chromosome that represents hyperparameters is fed into the kernel function of choice, and the SVR algorithm is trained with the training dataset. The RMSE value for every assessed chromosome was recorded, whereas the generated support vectors by the respective SVR algorithms were saved for later use

(c) Saved support vectors in step b are further employed for evaluating each SVR algorithm that has been trained with the help of the testing dataset and the chromosome that shows the least value of RMSE is saved

(d) Each developed model is evaluated with RMSE testing as obtained in c. The model with the least RMSE

value is chosen as the best, and the model with the highest RMSE value is considered the worst model

Step III. Reproduction phase: breeding of subsequent generation is achieved by selecting a fraction of the existing initial population. Selection of individual solutions is performed by using a fitness-based approach, and breeding of new populations with the best fitness is ensured by using a selection probability of 0.8

Step IV. Implementation of crossover operator: the crossover operator changes or modifies the chromosomal programming from one generation to the next. The probability of sexual crossover of 0.65 was implemented in this research work to replace weaker chromosomes in the population. Selection of offspring resulted in the exchange of sequences and portions of the parent chromosomes

Step V. Mutation operator: the mutation operator helps to maintain the diversity in genetics from one generation to the next. It also ensures that each gene has access to the entire range of alleles. In this work, distortion of solutions was prevented by adopting 0.009 probability of mutation for generating mutated offspring

Step VI. Replacement of population: the least-fit individuals in the population (as determined by the computed RMSE) are replaced by new individuals

Step VII. Stopping conditions: Step II to Step V were repeated for the newly generated population. The repetition continues and only stops when the value of RMSE-testing is zero or when the RMSE testing yields the same result after fifty consecutive iterations

## 4. Results and Discussion

This section discusses the results of the developed hybrid intelligent model. The results of the developed stepwise regression are also compared with intelligent-based models. Influence of model convergence on the population size is also presented.

*4.1. Optimizations of Intelligent-Based Model Parameters Using Genetic Evolutionary Optimization Algorithm.* Figure 1 is a presentation of the results of the evolved optimization genetic algorithm for finding the best values for SVR hyperparameters. The convergence of the regulation factor which regulates a trade-off between complexity and error minimization in the developed hybrid GA-SVR model is illustrated in Figure 1(a). The population sizes were adjusted between ten to one hundred as shown in Figure 1(a). For ten exploring numbers of chromosomes, the model converges to relatively high values of penalty factor.

When the size of population was increased to fifty for proper exploration and exploitation of the search space, the values of the penalty factor got reduced and global convergence was attained. Further increase in the size of chromosomes does not influence the model performance and convergence. The variation of the threshold error as measured by the hyperparameter epsilon with population size is presented in Figure 1(b). At a population size of ten, the model converges to a very low error threshold. However, model overfitting was observed. The overfitness disappeared when the population size changes to fifty due to optimization of the exploration and exploitation capacity of the model. Any increase in the size of the population beyond fifty brings no further development to the model performance. The parameter that influences transformation of data from a space to another through kernel trick was investigated at different population size and presented in Figure 1(c). Gaussian kernel function was used for the transformation, while the optimum size of the chromosomes for kernel parameter optimization is fifty as shown in the figure. The value of each of the intelligent-based model parameters is presented in Table 2.

The error convergence as the exploration and exploitation capacity of the model is altered at different iteration points and population size is presented in Figure 1(d). Premature and local convergences were observed for a population size of ten, while the model shows global convergence as the number of chromosomes exploring the space attained fifty.

*4.2. Computation and Comparison of the Performance of the Developed Models.* The empirical equation governing the implementation of the developed STRA model is presented in equation (4). Implementation of the stepwise regression-based empirical equation requires adequate knowledge of the distortion along the $a$-axis, $b$-axis, and $c$-axis due to the incorporated dopants.

$$\begin{aligned}\mathrm{STRA} = {} & 240.0888 - 55.8272a - 13.5334b \\ & - 22.7139c + 3.224602ab + 5.147369ac.\end{aligned} \tag{4}$$

Incorporation of foreign materials into the crystal structure of SnS semiconductor results in elongation or contraction in the crystal lattices of the semiconductor which are made used by the developed empirical equation for energy gap computation. To determine the energy gap of SnS semiconductor, the developed STRA model is compared to the developed hybrid intelligent GA-SVR model in terms of performance measuring parameters, utilizing mean absolute error (MAE), root mean square error (RMSE), and correlation coefficient (CC). The comparison of STRA and GA-SVR model in the training phase of model development using correlation coefficient is presented in Figure 2(a). As shown in Figure 2(a), the GA-SVR model has better performance than the STRA model, with a performance improvement of 47.06%. The comparison of GA-SVR and STRA models based on RMSE for the training set of data presented in Figure 2(b) shows 91.7% percentage improvement of GA-SVR over STRA model. Similar training phase comparison based on MAE is presented in Figure 2(c) in which the developed intelligent GA-SVR-based model outperforms STRA model with a performance enhancement of 92.70%.

Comparisons during the testing phase of model development are presented in Figures 2(d)–2(f) based on CC, RMSE, and MAE performance metrics, respectively. On these three bases, the developed GA-SVR model

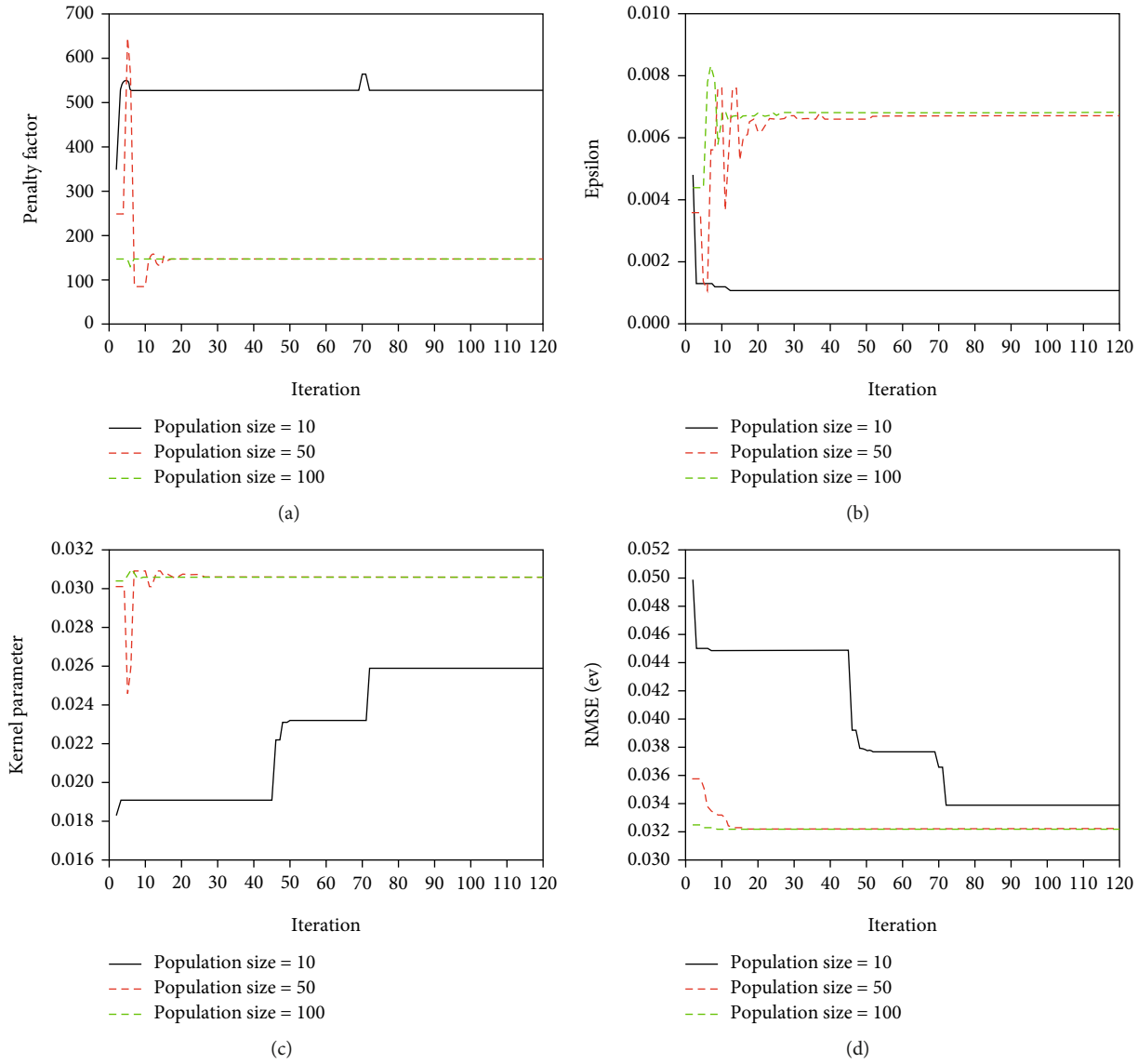


Figure 1: Optimization of model parameters using genetic algorithm. (a) Penalty factor convergence at various sizes of the population. (b) Epsilon convergence at various sizes of the population. (c) Gaussian kernel parameter convergence at various sizes of the population. (d) Error convergence at various sizes of the population.

Table 2: Optimum values of the intelligent model parameters.

| Intelligent model parameters | Optimum values |
|---|---|
| Penalty factor | 147.6952 |
| Function (kernel) | Gaussian |
| Error threshold epsilon | 0.0067 |
| Hyperplane lambda | E-7 |
| Kernel parameter | 0.0306 |
| Population size | 50 |

outperforms STRA model with 20.98%, 70.68%, and 67.63% improvements in performance, respectively. Table 3 presents the values of each of the performance evaluation parameters during the training and testing phases of model development. The table further presents the percentage improvement for each of the evaluation parameters at the training and testing stage of model development.

For further clarification on the performance superiority of the developed GA-SVR intelligent model and STRA model, a correlation cross-plot of the estimates of both models is presented in Figure 3. The estimates of GA-SVR model are perfectly aligned, while deviations characterize the results of the developed STRA model. The observed deviations of the outcomes of the developed STRA model may be due to the failure of the stepwise regression-based model to account for nonlinearity behavior characterizing the lattice parameter distortion in SnS semiconductor after foreign material incorporation. The developed intelligent-based model addresses the nonlinearity through convex

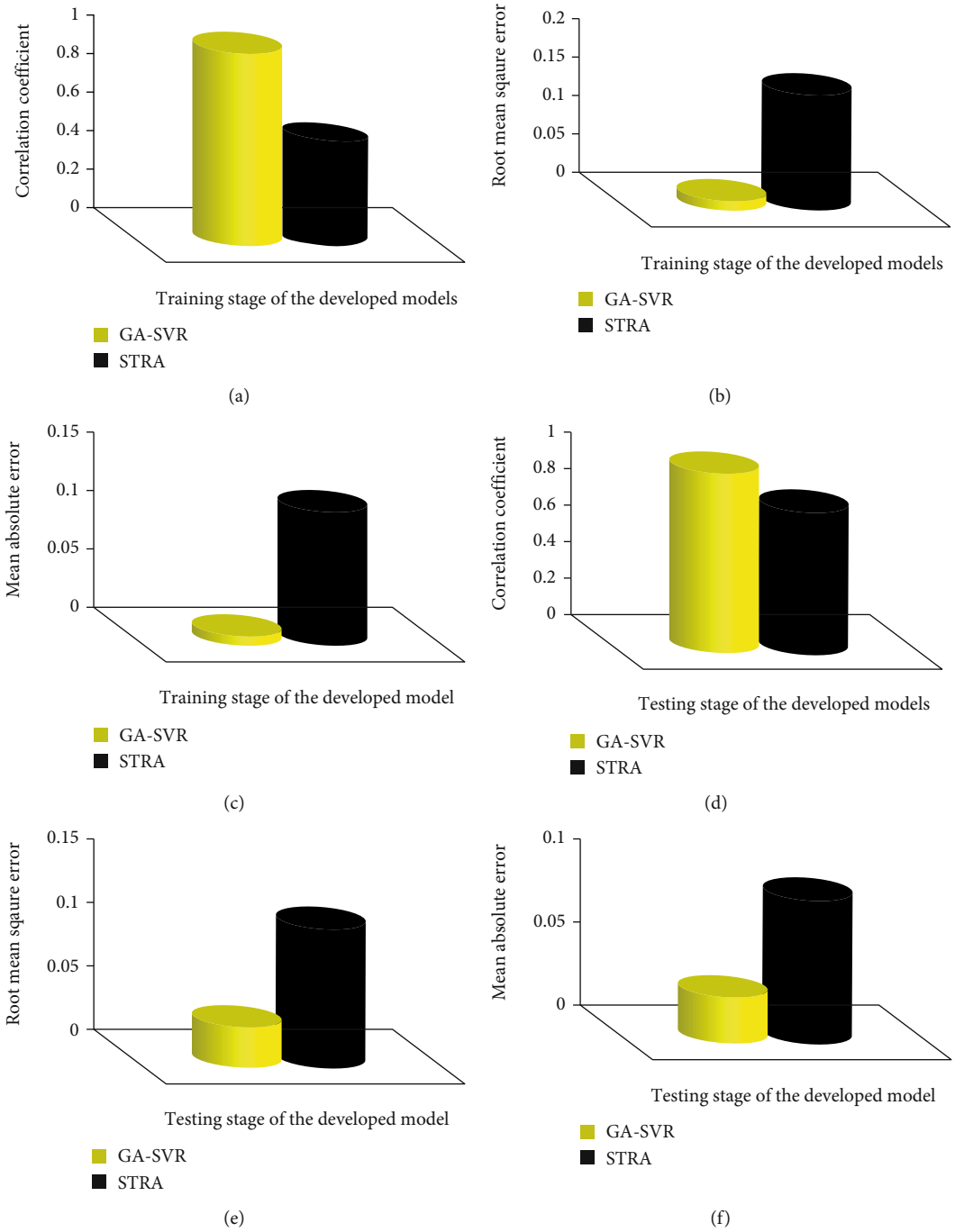


Figure 2: Performance comparison between the developed STRA model and intelligent (GA-SVR) based model. (a) Training performance comparison on the basis of correlation coefficient. (b) Training performance comparison on the basis of root mean square error. (c) Training performance comparison on the basis of mean absolute error. (d) Testing performance comparison on the basis of correlation coefficient. (e) Testing performance comparison on the basis of root mean square error. (f) Testing performance comparison on the basis of mean absolute error.

optimization procedures in SVR development, invocation of Lagrange multipliers, and hyperparameter optimization using genetic algorithm.

*4.3. Comparisons of Energy Gap of Doped SnS Semiconductors during Validation of the Developed Models.* The energy gaps of doped samples of SnS semiconductors are presented in Figures 4 and 5. The samples investigated and presented in this section were not included during the training phase of model development. The developed GA-SVR model only employs the support vectors obtained during the training processes for its prediction. Figure 4 presents the influence of indium and silver nanoparticle inclusion on the energy gaps of SnS semiconductor.

Lattice inclusion of indium and silver particles enhances faults and mismatch in lattice and ultimately leads to a

Table 3: Performance of the developed model as well as percentage improvement.

| | Training | | | Testing | | |
|---|---|---|---|---|---|---|
| | CC | RMSE | MAE | CC | RMSE | MAE |
| GA-SVR | 0.9978 | 0.0122 | 0.0084 | 0.9900 | 0.0322 | 0.0282 |
| STRA | 0.528262 | 0.1518 | 0.1151 | 0.7823 | 0.1098 | 0.0871 |
| % improvement of GA-SVR over STRA model | 47.05732 | 91.9628 | 92.7033 | 20.9817 | 70.6798 | 67.6319 |

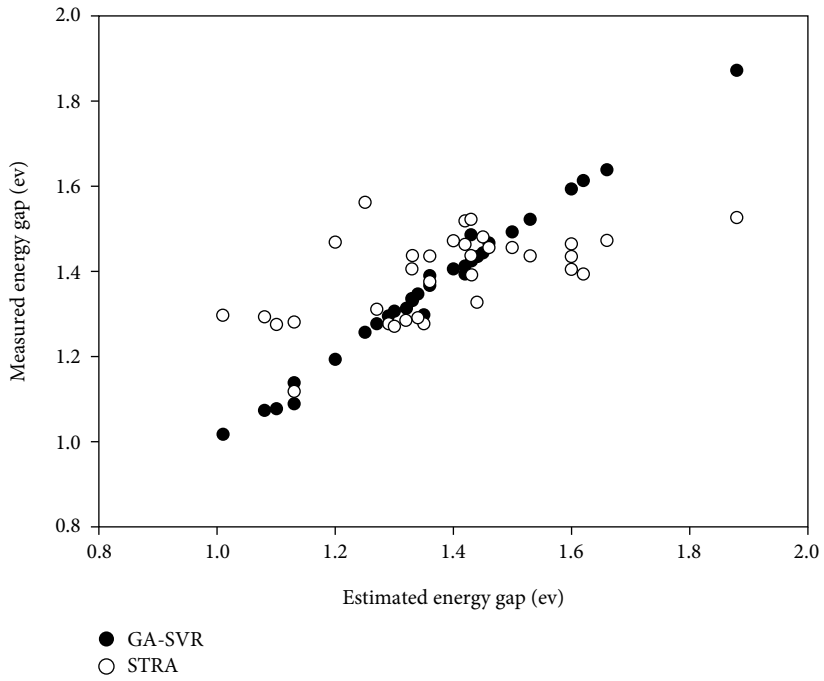


Figure 3: Correlation cross-plot between measured and estimated energy gap.

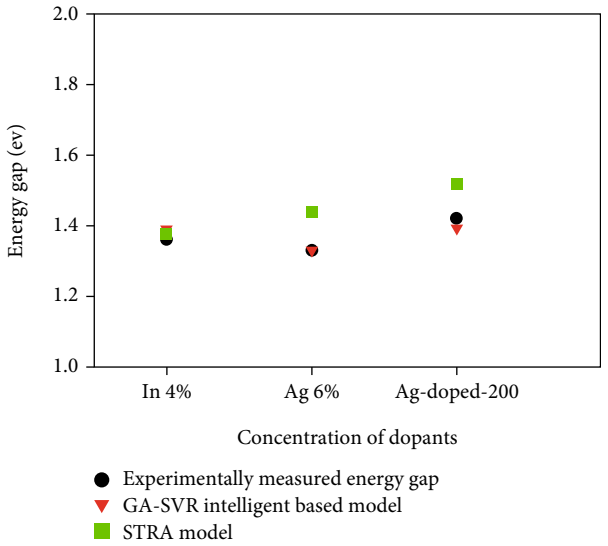


Figure 4: Influence of indium and silver dopants on energy gap of SnS semiconductor.

distortion in the crystal lattice. The observed distortion and lattice strain that influences the semiconductor energy gap can be attributed to the ionic radii difference between $Sn^{2+}$ of 9.3 nm and $In^{3+}$ of 8.0 nm.

Copper and indium incorporation presented in Figure 5 introduce band levels in SnS semiconductor close to the valence band which promotes conduction electrons from indium/copper at a wavelength lower than the required wavelength for electron movement from the valence to conduction bands. The sulfur vacancies due to the valence difference between $In^{3+}$ and $Sn^{2+}$ further enhance electron movement from conduction to the valence band. The energy gap of SnS semiconductor is expected to reduce as the grain sizes get reduced in accordance with quantum size effect since the quantum size becomes apparent when the grain sizes approach values smaller than 100 nm. Hybridization of valence and conduction bands as a result of dopants incorporation also influences the value of energy gap. The estimates of the developed STRA and GA-SVR models have excellent agreement with the measured values [31, 104, 108]. The deviations observed in the estimates of STRA model as compared with that of GA-SVR model may be attributed to the failure of STRA-based model to account for nonlinearity behavior existing between lattice distortion of doped

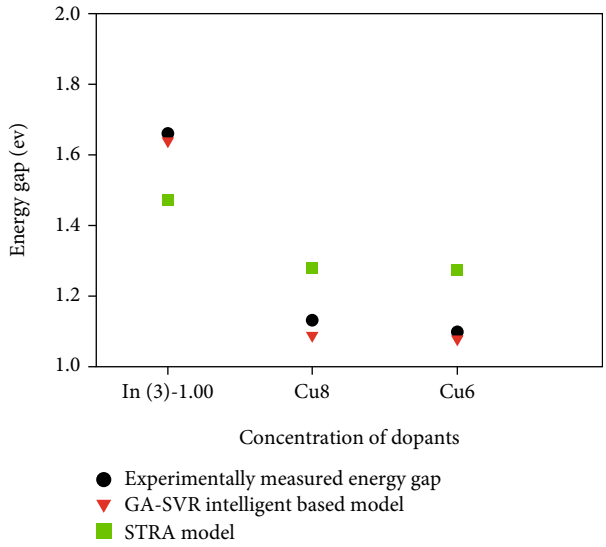


Figure 5: Effect of copper and indium dopants on the energy gap of SnS semiconductor.

SnS semiconductor and the energy gap. The mathematical background governing the implementation of the hybrid intelligent GA-SVR-based model, such as convex optimization implementation, Lagrange multipliers, and empirical risk implementation, further strengthens the potentiality and superiority of the intelligent model for effective capturing of the relationship between lattice distortion and the corresponding energy gap.

## 5. Conclusion

The band gap energy of the nanostructured SnS semiconductor incorporated with some dopants is modeled with stepwise-based regression algorithm (STRA) and hybrid intelligent-based genetic algorithm- (GA-) embedded support vector regression (SVR) algorithm. The developed models employ lattice parameters of distorted nanostructured semiconductor as model inputs. The developed GA-SVR model performs better than STRA model with performance improvement of 47.06%, 91.7%, and 92.70% during the training phase using the correlation coefficient, root mean square error, and mean absolute error as performance measuring yardsticks. The developed models further investigate the influence as well as the significance of indium, copper, and silver incorporation on lattice structure of SnS semiconductor and the obtained model estimates align perfectly with the measured energy gaps. The superiority of the intelligent-based model (GA-SVR) over stepwise regression-based model (STRA) can be attributed to the intrinsic mathematical background of the employed intelligent-based model which includes the implementation of Lagrange multipliers, convex optimization invocation, and employed empirical risk. The outcomes of the developed model provide an intelligent, fast, and cost-effective method of SnS energy gap characterization with a high degree of precision as well as experimental stress circumvention.

## Data Availability

The raw data needed to reproduce the findings of this study can be found in the cited references in Section3.1.

## Conflicts of Interest

Authors declare that there is no competing interest.

## Acknowledgments

The support received from Tertiary Education Trust Fund through Adekunle Ajasin University, Akungba Akoko, is well appreciated.

## References

[1] S. H. Chaki, M. D. Chaudhary, and M. P. Deshpande, "Effect of indium and antimony doping in SnS single crystals," *Materials Research Bulletin*, vol. 63, pp. 173–180, 2015.

[2] A. Basak, A. Mondal, and U. P. Singh, "Materials Science In Semiconductor Processing Impact of substrate temperature on the structural, optical and electrical properties of thermally evaporated SnS thin fi lms," *Materials Science in Semiconductor Processing*, vol. 56, pp. 381–385, 2016.

[3] L. Ren, Z. Jin, W. Wang et al., "Preparation and characterization of SnS nanocrystals by a triethanolamine- assisted diethylene glycol solution synthesis," *Applied Surface Science*, vol. 258, no. 4, pp. 1353–1358, 2011.

[4] D. Das and R. K. Dutta, "A Novel Method of Synthesis of Small Band Gap SnS Nanorods and Its Efficient Photocatalytic Dye Degradation," *Journal af Colloid and Interface Science*, vol. 457, pp. 339–344, 2015.

[5] F. A. Al-Agel and W. E. Mahmoud, "Synthesis and characterization of AIS chalcopyrite thin films for solar cell applications," *Materials Letters*, vol. 82, pp. 82–84, 2012.

[6] R. Caballero, V. Condé, and M. León, "SnS thin films grown by sulfurization of evaporated Sn layers: effect of sulfurization temperature and pressure," *Thin Solid Films*, vol. 612, pp. 202–207, 2016.

[7] F. A. Al-Agel and W. E. Mahmoud, "Synthesis and characterization of highly stoichiometric AgInSe2 thin films via a sol-gel spin-coating technique," *Journal of Applied Crystallography*, vol. 45, no. 5, pp. 921–925, 2012.

[8] J. A. A. M. Courel-piedrahita, "SnS-Based Thin Film Solar Cells : Perspectives over the Last 25 Years," *Journal of Materials Science: Materials in Electronics*, vol. 26, no. 7, pp. 4541–4556, 2015.

[9] C. Lu, Y. Zhang, L. Zhang, and Q. Yin, "Applied Surface Science Preparation and photoelectrochemical properties of SnS/SnSe and SnSe/SnS bilayer structures fabricated via electrodeposition," *Applied Surface Science*, vol. 484, pp. 560–567, 2019.

[10] M. Cheraghizade, F. Jamali-sheini, and P. Shabani, "Materials Science in Semiconductor Processing Annealing temperature of nanostructured SnS on the role of the absorber layer," *Materials Science in Semiconductor Processing*, vol. 90, pp. 120–128, 2019.

[11] S. Cheng, Y. He, G. Chen, E. C. Cho, and G. Conibeer, "Influence of EDTA concentration on the structure and properties of SnS films prepared by electro-deposition," *Surface and Coatings Technology*, vol. 202, no. 24, pp. 6070–6074, 2008.

[12] H. Kafashan, R. Ebrahimi-kahrizsangi, F. Jamali-sheini, R. Youse, I. The, and A. Sns, "Effect of Al doping on the structural and optical properties of electrodeposited SnS thin fi lms," *Physica Status Solidi (a)*, vol. 213, no. 5, pp. 1302–1308, 2016.

[13] V. S. R. R. Pullabhotla and M. W. Mabila, *Author' s Accepted Manuscript*, Elsevier, 2016.

[14] X. Xu, C. Takai, T. Shirai, and M. Fuji, "Synthesis and Characterization of a Novel Hollow Nanoparticle-Based SnS Crystal Product with Microcluster-like 3D Network Hierarchitectures," *Advanced Powder Technology*, vol. 26, no. 5, pp. 1327–1334, 2015.

[15] N. Maharjan, "Electronic band structure of TMDs," vol. 53, no. 9, pp. 1689–1699, 2013.

[16] H. Li, J. Ji, X. Zheng, Y. Ma, Z. Jin, and H. Ji, "Preparation of SnS quantum dots for solar cells application by an in-situ solution chemical reaction process," *Materials Science in Semiconductor Processing*, vol. 36, pp. 65–70, 2015.

[17] T. H. Sajeesh, A. R. Warrier, C. S. Kartha, and K. P. Vijayakumar, "Optimization of parameters of chemical spray pyrolysis technique to get n and p-type layers of SnS," *Thin Solid Films*, vol. 518, no. 15, pp. 4370–4374, 2010.

[18] M. Devika, N. K. Reddy, K. Ramesh, K. R. Gunasekhar, E. S. R. Gopal, and K. T. R. Reddy, "Low resistive micrometer-thick snS: Ag films for optoelectronic applications," *Journal of the Electrochemical Society*, vol. 153, no. 8, article G727, 2006.

[19] S. I. Son, D. Shin, Y. G. Son et al., "Effect of working pressure on the properties of RF sputtered SnS thin films and photovoltaic performance of SnS-based solar cells," *Journal of Alloys and Compounds*, vol. 831, article 154626, 2020.

[20] R. E. Banai, M. W. Horn, and J. R. S. Brownson, "A review of tin (II) monosulfide and its potential as a photovoltaic absorber," *Solar Energy Materials & Solar Cells*, vol. 150, pp. 112–129, 2016.

[21] R. E. Banai, H. Lee, M. A. Motyka et al., "Optical properties of sputtered SnS thin films for photovoltaic absorbers," *IEEE Journal of Photovoltaics*, vol. 3, no. 3, pp. 1084–1089, 2013.

[22] W. Shockley and H. J. Queisser, "Detailed balance limit of efficiency of p-n junction solar cells," *Journal of Applied Physics*, vol. 32, no. 3, pp. 510–519, 1961.

[23] H. S. Yun, B. W. Park, Y. C. Choi, J. Im, T. J. Shin, and S. I. Seok, "Efficient nanostructured TiO2/SnS heterojunction solar cells," *Advanced Energy Materials*, vol. 9, no. 35, article 1901343, 2019.

[24] P. Sinsermsuksakul, L. Sun, S. W. Lee et al., "Overcoming efficiency limitations of SnS-based solar cells," *Advanced Energy Materials*, vol. 4, no. 15, pp. 1–7, 2014.

[25] T. Sall, M. Mollar, and B. Marí, "Substrate influences on the properties of SnS thin films deposited by chemical spray pyrolysis technique for photovoltaic applications," *Journal of Materials Science*, vol. 51, no. 16, pp. 7607–7613, 2016.

[26] J. J. Loferski, "Theoretical considerations governing the choice of the optimum semiconductor for photovoltaic solar energy conversion," *Journal of Applied Physics*, vol. 27, no. 7, pp. 777–784, 1956.

[27] L. A. Burton and A. Walsh, "Band alignment in SnS thin-film solar cells: possible origin of the low conversion efficiency," *Applied Physics Letters*, vol. 102, no. 13, pp. 132111–132120, 2013.

[28] G. Gordillo, M. Botero, and J. S. Oyola, "Synthesis and study of optical and structural properties of thin films based on new photovoltaic materials," *Microelectronics Journal*, vol. 39, no. 11, pp. 1351–1353, 2008.

[29] A. Dussan, F. Mesa, and G. Gordillo, "Effect of substitution of Sn for Bi on structural and electrical transport properties of SnS thin films," *Journal of Materials Science*, vol. 45, no. 9, pp. 2403–2407, 2010.

[30] B. H. Baby and D. Bharathi Mohan, "Structural, optical and electrical studies of DC-RF magnetron co-sputtered Cu, In & Ag doped SnS thin films for photovoltaic applications," *Solar Energy*, vol. 194, pp. 61–73, 2019.

[31] B. H. Baby, A. M. Thomas, E. G. Amrutha, and D. Bharathi Mohan, "Enhancement of optoelectronic properties via substitutional doping of Cu, in and Ag in SnS nanorods for thin film photovoltaics," *Solar Energy*, vol. 205, pp. 446–455, 2020.

[32] S. Sebastian, I. Kulandaisamy, A. M. S. Arulanantham et al., "Influence of Al doping concentration on the optoelectronic chattels of SnS thin films readied by NSP," *Optical and Quantum Electronics*, vol. 51, no. 4, pp. 1–16, 2019.

[33] A. Javed, Qurat-ul-Ain, and M. Bashir, "Controlled growth, structure and optical properties of Fe-doped cubic $\pi$- SnS thin films," *Journal of Alloys and Compounds*, vol. 759, pp. 14–21, 2018.

[34] A. Akkari, M. Reghima, C. Guasch, and N. Kamoun-Turki, "Effect of copper doping on physical properties of nanocrystallized SnS zinc blend thin films grown by chemical bath deposition," *Journal of Materials Science*, vol. 47, no. 3, pp. 1365–1371, 2012.

[35] A. S. B. Ruyan and G. Rustum, "The perovskite structure – a review of its role in ceramic science and technology," *Materials Research Innovations*, vol. 4, pp. 3–26, 2000.

[36] K. Santhosh Kumar, C. Manoharan, S. Dhanapandian, and A. Gowri Manohari, "Effect of Sb dopant on the structural, optical and electrical properties of SnS thin films by spray pyrolysis technique," *Spectrochimica Acta Part A: Molecular and Biomolecular Spectroscopy*, vol. 115, pp. 840–844, 2013.

[37] B. Ghosh, R. Bhattacharjee, P. Banerjee, and S. Das, "Structural and optoelectronic properties of vacuum evaporated SnS thin films annealed in argon ambient," *Applied Surface Science*, vol. 257, no. 8, pp. 3670–3676, 2011.

[38] F. Y. Ran, Z. Xiao, Y. Toda, H. Hiramatsu, H. Hosono, and T. Kamiya, "N-type conversion of SnS by isovalent ion substitution: geometrical doping as a new doping route," *Scientific Reports*, vol. 5, pp. 1–8, 2015.

[39] A. Tanuševski and D. Poelman, "Optical and photoconductive properties of SnS thin films prepared by electron beam evaporation," *Solar Energy Materials & Solar Cells*, vol. 80, no. 3, pp. 297–303, 2003.

[40] W. Wang, K. K. Leung, W. K. Fong et al., "Molecular beam epitaxy growth of high quality p-doped SnS van der Waals epitaxy on a graphene buffer layer," *Journal of Applied physics*, vol. 111, no. 9, article 093520, 2012.

[41] M. Ichimura, K. Takeuchi, Y. Ono, and E. Arai, "Electrochemical deposition of SnS thin films," *Thin Solid Films*, vol. 361, pp. 98–101, 2000.

[42] K. Takeuchi, M. Ichimura, E. Arai, and Y. Yamazaki, "SnS thin films fabricated by pulsed and normal electrochemical deposition," *Solar Energy Materials & Solar Cells*, vol. 75, no. 3–4, pp. 427–432, 2003.

[43] R. Mariappan, T. Mahalingam, and V. Ponnuswamy, "Preparation and characterization of electrodeposited SnS thin films," *Optik*, vol. 122, no. 24, pp. 2216–2219, 2011.

[44] S. Cheng, Y. Chen, C. Huang, and G. Chen, "Characterization of SnS films prepared by constant-current electro-deposition," *Thin Solid Films*, vol. 500, no. 1–2, pp. 96–100, 2006.

[45] N. R. Mathews, "Charge transport in a pulseelectrodeposited SnS/Al Schottky device," *Semiconductor Science and Technology*, vol. 25, no. 10, article 105010, 2010.

[46] M. Devika, N. K. Reddy, F. Patolsky, K. Ramesh, and K. R. Gunasekhar, "Temperature dependent structural properties of nanocrystalline SnS structures," *Applied Physics Letters*, vol. 95, no. 26, pp. 2012–2015, 2009.

[47] R. W. Miles, O. E. Ogah, G. Zoppi, and I. Forbes, "Thermally evaporated thin films of SnS for application in solar cell devices," *Thin Solid Films*, vol. 517, no. 17, pp. 4702–4705, 2009.

[48] P. Sinsermsuksakul, J. Heo, W. Noh, A. S. Hock, and R. G. Gordon, "Atomic layer deposition of tin monosulfide thin films," *Advanced Energy Materials*, vol. 1, no. 6, pp. 1116–1125, 2011.

[49] K. Hartman, J. L. Johnson, M. I. Bertoni et al., "SnS thin-films by RF sputtering at room temperature," *Thin Solid Films*, vol. 519, no. 21, pp. 7421–7424, 2011.

[50] Z. Xu and Y. Chen, "Fabrication of SnS thin films by a novel multilayer-based solid-state reaction method," *Semiconductor Science and Technology*, vol. 27, no. 3, article 035007, 2012.

[51] A. Sánchez-Juárez, A. Tiburcio-Silver, and A. Ortiz, "Fabrication of SnS2/SnS heterojunction thin film diodes by plasma-enhanced chemical vapor deposition," *Thin Solid Films*, vol. 480, pp. 452–456, 2005.

[52] S. A. Bashkirov, V. F. Gremenok, V. A. Ivanov, V. V. Lazenka, and K. Bente, "Tin sulfide thin films and Mo/p-SnS/n-CdS/ZnO heterojunctions for photovoltaic applications," *Thin Solid Films*, vol. 520, no. 17, pp. 5807–5810, 2012.

[53] D. Avellaneda, G. Delgado, M. T. S. Nair, and P. K. Nair, "Structural and chemical transformations in SnS thin films used in chemically deposited photovoltaic cells," *Thin Solid Films*, vol. 515, no. 15, pp. 5771–5776, 2007.

[54] M. T. S. Nair, C. Lopéz-Mata, O. Gomez Daza, and P. K. Nair, "Copper tin sulfide semiconductor thin films produced by heating SnS-CuS layers deposited from chemical bath," *Semiconductor Science and Technology*, vol. 18, no. 8, pp. 755–759, 2003.

[55] C. Gao, H. Shen, and L. Sun, "Preparation and properties of zinc blende and orthorhombic SnS films by chemical bath deposition," *Applied Surface Science*, vol. 257, no. 15, pp. 6750–6755, 2011.

[56] E. Turan, M. Kul, A. S. Aybek, and M. Zor, "Structural and optical properties of SnS semiconductor films produced by chemical bath deposition," *Journal of Physics D: Applied Physics*, vol. 42, no. 24, article 245408, 2009.

[57] U. Chalapathi, B. Poornaprakash, and S. H. Park, "Growth and properties of cubic SnS films prepared by chemical bath deposition using EDTA as the complexing agent," *Journal of Alloys and Compounds*, vol. 689, pp. 938–944, 2016.

[58] U. Chalapathi, B. Poornaprakash, and S. H. Park, "Effect of post-deposition annealing on the growth and properties of cubic SnS films," *Superlattices and Microstructures*, vol. 103, pp. 221–229, 2017.

[59] T. H. Sajeesh, K. B. Jinesh, C. S. Kartha, and K. P. Vijayakumar, "Role of pH of precursor solution in taming the material properties of spray pyrolysed SnS thin films," *Applied Surface Science*, vol. 258, no. 18, pp. 6870–6875, 2012.

[60] N. Koteswara Reddy and K. T. Ramakrishna Reddy, "Growth of polycrystalline SnS films by spray pyrolysis," *Thin Solid Films*, vol. 325, no. 1–2, pp. 4–6, 1998.

[61] K. T. Ramakrishna Reddy, P. Purandar Reddy, R. W. Miles, and P. K. Datta, "Investigations on SnS films deposited by spray pyrolysis," *Optical Materials*, vol. 17, no. 1–2, pp. 295–298, 2001.

[62] K. T. Ramakrishna Reddy, N. Koteswara Reddy, and R. W. Miles, "Photovoltaic properties of SnS based solar cells," *Solar Energy Materials & Solar Cells*, vol. 90, no. 18–19, pp. 3041–3046, 2006.

[63] N. K. Reddy and K. T. R. Reddy, "SnS films for photovoltaic applications: physical investigations on sprayed SnxSy films," *Physica B: Condensed Matter*, vol. 368, no. 1–4, pp. 25–31, 2005.

[64] M. R. Fadavieslam, N. Shahtahmasebi, M. Rezaee-Roknabadi, and M. M. Bagheri-Mohagheghi, "A study of the photoconductivity and thermoelectric properties of Sn xSy optical semiconductor thin films deposited by the spray pyrolysis technique," *Physica Scripta*, vol. 84, no. 3, article 035705, 2011.

[65] B. Ghosh, M. Das, P. Banerjee, and S. Das, "Fabrication of SnS thin films by the successive ionic layer adsorption and reaction (SILAR) method," *Semiconductor Science and Technology*, vol. 23, no. 12, article 125013, 2008.

[66] B. Ghosh, M. Das, P. Banerjee, and S. Das, "Fabrication and optical properties of SnS thin films by SILAR method," *Applied Surface Science*, vol. 254, no. 20, pp. 6436–6440, 2008.

[67] B. Ghosh, S. Chowdhury, P. Banerjee, and S. Das, "Fabrication of CdS/SnS heterostructured device using successive ionic layer adsorption and reaction deposited SnS," *Thin Solid Films*, vol. 519, no. 10, pp. 3368–3372, 2011.

[68] B. Subramanian, C. Sanjeeviraja, and M. Jayachandran, "Photoelectrochemical characteristics of brush plated tin sulfide thin films," *Solar Energy Materials & Solar Cells*, vol. 79, no. 1, pp. 57–65, 2003.

[69] V. N. Vapnik, *Statistical Learning Theory*, Wiley-Interscience, New York, New York, USA, 1998.

[70] H. B. Adeyemo, T. O. Owolabi, M. A. Suleiman et al., "Heliyon hybrid chemometric approach for estimating the heat of detonation of aromatic energetic compounds," *Heliyon*, vol. 5, no. 7, article e02035, 2019.

[71] K. O. Akande, S. O. Olatunji, T. O. Owolabi, and A. AbdulRaheem, "Comparative analysis of feature selection-based machine learning techniques in reservoir characterization," in *Paper presented at the SPE Saudi Arabia Section Annual Technical Symposium and Exhibition*, pp. 1–12, Al-Khobar, Saudi Arabia, April 2015.

[72] K. O. Akande, S. O. Olatunji, T. O. Owolabi, and A. AbdulRaheem, "Feature selection-based ANN for improved characterization of carbonate reservoir," in *Paper presented at the SPE Saudi Arabia Section Annual Technical Symposium and Exhibition*, Al-Khobar, Saudi Arabia, April 2015.

[73] K. O. Akande, T. O. Owolabi, and S. O. Olatunji, "Investigating the Effect of Correlation-Based Feature Selection on the Performance of Neural Network in Reservoir Characterization,"

*Journal of Natural Gas Science and Engineering*, vol. 27, pp. 98–108, 2015.

[74] H. Kwon and B. M. Wong, "A Machine Learning Approach for Predicting Defluorination of Per- and Polyfluoroalkyl Substances (PFAS) for Their Efficient Treatment and Removal," *Environmental Science & Technology Letters*, vol. 6, no. 10, pp. 624–629, 2019.

[75] A. S. Christensen, F. R. Rasmussen, and J. Elm, "Quantum Machine Learning Approach for Studying Atmospheric Cluster Formation," *Environmental Science & Technology Letters*, vol. 9, no. 3, pp. 239–244, 2022.

[76] O. E. Olubi, E. O. Oniya, and T. O. Owolabi, "Development of predictive model for radon-222 estimation in the atmosphere using stepwise regression and grid search based-random forest regression," *Journal of the Nigerian Society of Physical Sciences*, vol. 3, pp. 132–139, 2021.

[77] T. O. Owolabi, "Development of a particle swarm optimization based support vector regression model for titanium dioxide band gap characterization," *Journal of Semiconductors*, vol. 40, no. 2, article 022803, 2019.

[78] S. O. Olatunji and T. O. Owolabi, "Modeling superconducting transition temperature of doped MgB 2 superconductor from structural distortion and ambient temperature resistivity measurement using hybrid intelligent approach," *Computational Materials Science*, vol. 192, article 110392, 2021.

[79] S. M. I. Shamsah and T. O. Owolabi, "Newtonian mechanics based hybrid machine learning method of characterizing energy band gap of doped zno semiconductor," *Chinese Journal of Physics*, vol. 68, pp. 493–506, 2020.

[80] A. A. Akinpelu, M. Ali, T. O. Owolabi et al., "A support vector regression model for the prediction of total polyaromatic hydrocarbons in soil: an artificial intelligent system for mapping environmental pollution," *Neural Computing and Applications*, vol. 32, no. 18, pp. 14899–14908, 2020.

[81] T. O. Owolabi, K. O. Akande, S. O. Olatunji, and N. Aldhafferi, "Ensemble-based support vector regression with gravitational search algorithm optimization for estimating magnetic relative cooling power of manganite refrigerant in magnetic refrigeration application," *Journal of Superconductivity and Novel Magnetism*, vol. 32, no. 7, pp. 2107–2118, 2019.

[82] V. Vapnik, *The Nature of Statistical Learning Theory*, Springer, New York, 1995.

[83] L. M. Schmitt, "Theory of genetic algorithms," *Theoretical Computer Science*, vol. 259, no. 1–2, pp. 1–61, 2001.

[84] A. A. Adewumi, M. Ismail, M. A. M. Ariffin et al., "Empirical modelling of the compressive strength of an alkaline activated natural pozzolan and limestone powder mortar," *Ceramics-Silikaty*, vol. 64, no. 4, pp. 407–417, 2020.

[85] V. N. Vapnik, "An overview of statistical learning theory," *IEEE Transactions on Neural Networks*, vol. 10, no. 5, pp. 988–999, 1999.

[86] M. Ghorbani, G. Zargar, and H. Jazayeri-Rad, "Prediction of asphaltene precipitation using support vector regression tuned with genetic algorithms," *Petroleum*, vol. 2, no. 3, pp. 301–306, 2016.

[87] A. A. Adewumi, T. O. Owolabi, I. O. Alade, and S. O. Olatunji, "Estimation of physical, mechanical and hydrological properties of permeable concrete using computational intelligence approach," *Applied Soft Computing*, vol. 42, pp. 342–350, 2016.

[88] T. A. Oyehan, I. O. Alade, A. Bagudu, K. O. Sulaiman, S. O. Olatunji, and T. A. Saleh, "Predicting of the refractive index of haemoglobin using the hybrid GA-SVR approach," *Computers in Biology and Medicine*, vol. 98, pp. 85–92, 2018.

[89] D. Parbat and M. Chakraborty, "A python based support vector regression model for prediction of COVID19 cases in India," *Chaos,Solitons and Fractals*, vol. 138, article 109942, 2020.

[90] T. O. Owolabi, M. A. Suleiman, H. B. Adeyemo, K. O. Akande, J. Alhiyafi, and S. O. Olatunji, "Estimation of minimum ignition energy of explosive chemicals using gravitational search algorithm based support vector regression," *Journal of Loss Prevention in the Process Industries*, vol. 57, pp. 156–163, 2019.

[91] T. O. Owolabi, K. O. Akande, S. O. Olatunji, N. Aldhafferi, and A. Alqahtani, "Support vector regression ensemble for effective modeling of magnetic ordering temperature of doped manganite in magnetic refrigeration," *Journal of Low Temperature Physics*, vol. 195, no. 1–2, pp. 179–201, 2019.

[92] P. Chibuike, S. Ogochukwu, and T. O. Owolabi, "Perovskite tetragonality modeling for functional properties enhancement using Newtonian search based support vector regression computational method," *Journal of the Nigerian Society of Physical Sciences*, vol. 4, pp. 20–26, 2022.

[93] J. Wu and Y. Wang, "A working likelihood approach to support vector regression with a data-driven insensitivity parameter," 2020, http://arxiv.org/abs/2003.03893.

[94] M. Awad and R. Khanna, *Efficient Learning Machines: Theories, Concepts, and Applications for Engineers and System Designers*, Springer Nature, Berlin Germany, 2015.

[95] D. Whitley, "A genetic algorithm tutorial," *Statistics and Computing*, vol. 4, no. 2, pp. 65–85, 1994.

[96] J. H. Holland, "Genetic algorithms and adaptation," vol. 16 of NATO Conf. Ser. II Syst. Sci., pp. 317–333, 1984.

[97] H. T. Do, N. Van Bach, L. Van Nguyen, H. T. Tran, and M. T. Nguyen, "A design of higher-level control based genetic algorithms for wastewater treatment plants," *Engineering Science and Technology, an International Journal*, vol. 24, no. 4, pp. 872–878, 2021.

[98] L. Shu, J. Sunarso, S. S. Hashim, J. Mao, W. Zhou, and F. Liang, "Advanced perovskite anodes for solid oxide fuel cells: a review," *International Journal of Hydrogen Energy*, vol. 44, no. 59, pp. 31275–31304, 2019.

[99] J. Wen, H. Yang, X. Tong, K. Li, S. Wang, and Y. Li, "Optimization investigation on configuration parameters of serrated fin in plate-fin heat exchanger using genetic algorithm," *International Journal of Thermal Sciences*, vol. 101, no. 2016, pp. 116–125, 2016.

[100] L. Gharsalli and Y. Guérin, "Composites Part C : Open Access Mechanical sizing of a composite launcher structure by hybridizing a genetic algorithm with a local search method," *Composites Part C Open Access*, vol. 5, article 100125, 2021.

[101] H. Chen, S. Liu, R. M. Magomedov, and A. A. Davidyants, "Optimization of inflow performance relationship curves for an oil reservoir by genetic algorithm coupled with artificial neural-intelligence networks," *Energy Reports*, vol. 7, pp. 3116–3124, 2021.

[102] Z. Guo, Y. Yao, J. Kong et al., "Accuracy analysis of international reference ionosphere 2016 and NeQuick2 in the Antarctic," *Sensors*, vol. 21, article 1551, 2021.

[103] A. Cevik, M. T. Gög, H. Güzelbey, and H. Filiz, "Advances in Engineering Software A new formulation for longitudinally stiffened webs subjected to patch loading using stepwise regression method," *Advances in Engineering Software*, vol. 41, pp. 611–618, 2010.

[104] B. H. Baby and A. Philipson, "Optik Temperature-assisted mechanochemically synthesized Cu and In doped SnS nanoparticles for thin film photovoltaics : structure, phase stability and optoelectronic properties," *Optik*, vol. 240, article 166848, 2021.

[105] A. Jafari-rad and H. Kafashan, "Preparation and characterization of electrochemically deposited nanostructured Ti-doped ZnS thin films," *Ceramics International*, vol. 45, no. 17, pp. 21413–21422, 2019.

[106] S. D. López-martínez, I. Juárez-ramírez, L. M. Torres-martínez, P. Babar, A. Lokhande, and J. Hyeok, "Chemistry SnS-AuPd thin fi lms for hydrogen production under solar light simulation," *Journal of Photochemistry and Photobiology A: Chemistry*, vol. 361, pp. 19–24, 2018.

[107] A. Boubakri, A. Jouidri, Y. Koumya, A. Rajira, A. Almaggoussi, and A. Abounadi, "Materials Today : Proceedings Chelating agent effect on optical properties of SnS films and an output characteristics simulation of based solar cells," *Materials Today: Proceedings*, vol. 51, pp. 2047–2052, 2021.

[108] V. K. Arepalli, S. J. Kim, and J. Kim, "Influence of substrate temperature on the growth properties of Ag-doped SnS films deposited by sputtering method," *Journal of Physics and Chemistry of Solids*, vol. 155, article 110099, 2021.

[109] K. S. Kumar, C. Manoharan, S. Dhanapandian, A. G. Manohari, and T. Mahalingam, "Optik Effect of indium incorporation on properties of SnS thin films prepared by spray pyrolysis," *Optik*, vol. 125, no. 15, pp. 3996–4000, 2014.

[110] M. Patel, I. Mukhopadhyay, and A. Ray, "Annealing influence over structural and optical properties of sprayed SnS thin films," *Optical Materials*, vol. 35, no. 9, pp. 1693–1699, 2013.